MOLEKUL
eISSN: 2503-0310

Articles
https://doi.org/10.20884/1.jm.2024.19.3.11056

Preparation of Proton-Conducting Solid Electrolyte Membrane Based on Carboxymethyl Chitosan Complexed with Ammonium Acetate

Nila Tanyela Berghuis[1]*, Shanny Fridarima[1], Elvira Nur Rachmadhanti[1], Sudaryanto[2], Sun Theo Constan Lotebulo Ndruru[3]*

[1]Department of Chemistry, Faculty of Science and Computer, Universitas Pertamina, Jl. Teuku Nyak Arief, Jakarta 12220, Indonesia
[2]Research Center for Advanced Materials, The National Research, and Innovation Agency of Indonesia, PUSPIPTEK Area Serpong, Tangerang Selatan, Banten 15314, Indonesia
[3]Research Center for Chemistry, The National Research and Innovation Agency of Indonesia, PUSPIPTEK Area Serpong, Tangerang Selatan, Banten 15314, Indonesia

*Corresponding author email: nila.tanyela@universitaspertamina.ac.id and sunt002@brin.go.id

Received January 15, 2024; **Accepted** October 07, 2024; **Available online** November 20, 2024

ABSTRACT. This research aims to prepare the proton-conducting solid electrolyte membrane based on carboxymethyl chitosan (CMCh) complexed with ammonium acetate (CH_3COONH_4). The membranes were prepared by using casting solution technique where the various weight percentages of ammonium acetate mixed to CMCh for obtaining optimum condition based on ionic conductivity analysis. Some characterizations were conducted to analysis the functional groups (involving complexation studies), ionic conductivities, mechanical properties, crystallinities, and thermal analysis by using FTIR, EIS, tensile tester, XRD, and TGA. The results showed that the optimum proton conductivity was obtained at the addition of 40% (w/w) CH_3COONH_4 salt as high as 1.39×10^{-4} S/cm and a tensile strength of 9.06 MPa. Based on the results, it can be concluded that the optimum condition of the membrane shows good characteristics to be applied as a proton conducting solid electrolyte.

Keywords: Ammonium acetate, carboxymethyl chitosan, polymer electrolyte, proton conductivity, proton-conducting membrane.

INTRODUCTION

The availability decrement of fossil fuels and the environmental problems they impact have driven the development of energy storage and conversion technologies such as supercapacitors, fuel cells, and electrochemical double-layer capacitors (EDLC) (Boopathi et al., 2017; Dannoun et al., 2022; Nayla & Radiman, 2023; Sihombing et al., 2023). Currently, many technological developments require energy storage devices such as rechargeable batteries as a source of energy (Ahmed & Abdullah, 2020).

Lithium-ion batteries are the most popular energy storage devices today due to their advantages, including relatively high energy density and long life cycle than other types of batteries (Han et al., 2021; Jiang et al., 2021; Singh et al., 2021; Yuan et al., 2022). However, the electrolyte source derived from lithium salts is costly, causing research to shift to the search for electrolyte sources from cheaper salts such as sodium salts, potassium salts, and ammonium salts (proton conductors) (Aziz et al., 2021; Chandra et al., 2016; Martinez-Cisneros et al., 2023; Nuryanto et al., 2013; Tahir et al., 2022). When compared to other ions, protons (H^+ ions) are the smallest ions and are therefore preferred to replace lithium ions, as they offer greater energy density (Alias et al., 2017; Heidari et al., 2018; Xu et al., 2022; J.-L. Yang et al., 2022)

Based on the previous explanation, proton batteries are a candidate for replacing lithium-ion batteries. In proton batteries, the electrolyte source comes from salts that can dissociate protons, especially from ammonium salts such as ammonium tetrafluoroborate, ammonium iodide, ammonium hexafluorophosphate, ammonium fluoride and ammonium acetate (Abdullah et al., 2021; Aziz et al., 2020; Hadi et al., 2022; Lakshmi et al., 2021).

The electrolyte is one of the crucial components in lithium-ion batteries. Generally, the rechargeable batteries' electrolyte still uses liquid (Septiana et al., 2019). Using liquid electrolytes provides advantages in high ion conductivity but poor safety aspects. Liquid electrolytes are flammable because the solvent used has a low boiling point, corrosive, not environmentally friendly, and others (Huy et al., 2021; Jian et al., 2022; Pratiwi, 2018; Varzi et al., 2016; Yao et al., 2019).

Using solid electrolytes to replace liquid electrolytes in rechargeable batteries, including proton batteries, offers advantages, excellent mechanical stability and thermal (Yusof et al., 2014). Solid electrolytes have at least two main components: polymer and electrolyte (salt). The choice of polymer type largely determines the performance of the solid electrolyte. Some common synthetic polymers that are widely used as the main matrix of solid electrolytes include polyethylene (PE), polypropylene (PP), polyethylene oxide (PEO), polyvinyl alcohol (PVA), polyvinylidene fluoride (PVDF), polymethyl methacrylate (PMMA) (Babiker et al., 2023; Hosseinioun & Paillard, 2020; Manoharan et al., 2021; Putri et al., 2021; Qiu et al., 2019; Xie et al., 2021; Zhu et al., 2021). However, the impact of using these polymers on the environment by industrial-scale fabrication processes and using synthetic polymers must be minimized.

Biopolymers can be used as an alternative to synthetic polymers as solid electrolyte polymer hosts because they have advantages over synthetic polymers, such as offering many polar functional groups such as -O-, -OH, -C=O, -NH_2, and others as transit sites for migrating ions. These functional groups can easily interact to form van der Waals, Coulomb, and hydrogen bond interactions that cannot be found in a single synthetic polymer (Francis et al., 2020; Lizundia & Kundu, 2021; Schlemmer et al., 2021).

Carboxymethyl chitosan is a chitosan-derived compound produced by substituting carboxymethyl groups on amine and hydroxyl groups (Miao et al., 2008; Suseno et al., 2017). Successful research reported that using carboxymethyl chitosan as a solid electrolyte membrane is a complex supercapacitor of potassium tetraborate and potassium carbonate (Cai et al., 2023). Carboxymethyl chitosan has advantages in terms of conductivity compared to the original compound (chitosan). Based on previous research, chitosan has a conductivity value of 2.93×10^{-9}S/cm lower than carboxymethyl chitosan, which is 2.20×10^{-7}S/cm (Shamsudin et al., 2020).

To increase the conductivity value of carboxymethyl chitosan, modification is carried out by doping ammonium acetate salt as a proton source (H^+) (Alias et al., 2017). It is known that ammonium salts can increase proton conductivity in carboxymethyl cellulose polymer electrolytes (Brza et al., 2020). Ammonium acetate is a plasticizer because it can increase amorphous properties and reduce the glass transition temperature in solid electrolytes (Pahune, 2011). Based on this background, this research was conducted to make a carboxymethyl chitosan solid electrolyte membrane complexed with ammonium acetate salt. The proton-conducting solid electrolyte membrane in this study was characterized using Fourier Transform Infra-Red (FTIR), Electrochemical Impedance Spectroscopy (EIS), tensile tester, X-ray Diffraction (XRD), and Thermogravimetry Analysis (TGA).

EXPERIMENTAL SECTION

Materials and Instruments

The chemicals used were carboxymethyl chitosan (commercial), ammonium acetate (Loba-Chemie, p.a), methanol (Merck, p.a), and aquades. The instruments used were FTIR (Thermoscientific, type Nicolet IS5), Electrochemical Impedance Spectroscopy (EIS, HIOKI, type *3532-50* LCR HiTESTER), *tensile tester* (AGS-X) and Thermogravimetry Analysis (TGA, SETARAM Thermal Analyzer Labsys Evo S60).

Preparation CMCh + AmAc salt-based Solid Electrolyte Membrane

The CMCh-based solid electrolyte membranes doped with AmAc salt were prepared using a casting solution technique. CMCh and AmAc salt were dissolved in aquades. The mixture was stirred for 24 h to obtain a homogenous solution. The solutions were poured onto the petri dish and vapored at 60°C in the oven for 24 h. The solid electrolyte membranes were prepared by comparing between CMCh and AmAc as follows, i.e. (100:0), (90:10), (80:20), (70:30), (60:40), (50:50) %w/w.

Characterizations

All of them were characterized using Fourier Transform Infrared (FTIR), ElectrochemicalImpedance Spectroscopy (EIS), tensile tester, X-ray Diffraction (XRD), and Thermogravimetry Analysis (TGA).

Molecular Structure Elucidation

Molecular structure analysis was conducted by using Nuclear Magnetic Resonance (NMR, JEOL) with a frequency of 500 MHz.

Functional Groups Analysis

Functional groups were characterized for membrane materials (carboxymethyl chitosan and ammonium acetate) and solid electrolyte membranes using Thermo Scientific type FTIR. The solid electrolyte membrane characterization was carried out using Fourier Transform Infra-Red Attenuated Total Reflection (FTIR-ATR) with a wave number range of 500-4000 cm^{-1} (Hadi, Aziz, Brza et al., 2022; Singh et al., 2020).

Percentage of Free Ions and Contact Ions

The FTIR deconvolution carried out the determination of the percentage of free ions. The calculation uses the following equation (Mejenom et al., 2018):

$$\text{Free ions}(\%) = \frac{A_f}{A_f + A_c} \times 100\% \quad (1)$$

$$\text{Contact ion}(\%) = 100 - \text{free ions} \quad (2)$$

Where A_f is the area under the peak for free ions, and A_c is the area under the peak for contact ions.

Ion Transport Parameters

Ion transport analysis includes density (η), ionic mobility (μ), and diffusion coefficient (D). The calculation uses the following equation (Abdalrahman et al., 2022):

$$\eta = \frac{M \times N_A \times free\ ions\ (\%)}{V_{total}} \quad (4)$$

$$\mu = \frac{\sigma}{\eta e} \quad (5)$$

$$D = \left(\frac{kT\mu}{e}\right) \quad (6)$$

Where M is moles of salt used, N_A is Avogadro number (6.02×10^{-23} mol^{-1}), V_{total} is total volume of solvent used for solid electrolyte membrane preparation, σ is proton conductivity of solid electrolyte membrane, e is electric charge (1.602×10^{-19} C), k is Boltzman constant (1.38×10-23 JK^{-1}) and T is absolute temperature (273 K).

Force Constant

The force constant (k) can be calculated using Hooke's law through the following equation (Akhtar et al., 2019; Hazaana et al., 2023):

$$v = \frac{1}{2\pi c}\sqrt{\frac{k}{\mu}}\ \text{N/cm} \quad (7)$$

$$k = 4\pi^2 c^2 v^2 \mu \quad (8)$$

$$\mu = \frac{m_1 \times m_2}{m_1 + m_2} \quad (9)$$

where v is wavenumber (cm^{-1}), c is the velocity of light (2.998×108 m.s^{-1}), k is force constant (N/cm), μ is reduced mass, and $\pi = 3{,}14$.

Absorption Bandwidth and Transmittance Intensity

Widening of the absorption band and the length of transmittance intensity in IR spectra can be calculated with the following equation (Hafiza & Isa, 2017):

$$Bandwidth\ (cm^{-1}) = B_t - B_0 \quad (10)$$

$$T\% = T_{baseline} - T_{puncak} \quad (11)$$

where B_t is the final baseline, and B_0 is the initial baseline.

Proton Conductivities Analysis

Proton conductivity measurements of each sample were carried out using electrochemical impedance spectroscopy (EIS, HIOKI, type 3532-50 LCR HiTESTER) in the frequency range 42 Hz-1 MHz at room temperature. The samples were sandwiched with stainless steel electrodes connected to the LCR tester (Hemalatha et al., 2021; Mahalakshmi et al., 2019; Rahamathullah et al., 2020). Rahamathullah et al (2020) mentioned that the calculation of bulk proton conductivity could be done with the following equation (Rahamathullah et al., 2020):

$$\sigma = \frac{t}{R_b \times A} \quad (12)$$

Where σ is bulk proton conductivity (S/cm), t is the thickness (cm), A is the surface area of the electrode contact area with the membrane (cm^2), and R_b is bulk resistance (ohm).

Alfannakh and Ibrahim (2022) suggest that EIS test results can be utilized to calculate proton conductivity using Jonscher's Power Law equation, which can be done using OriginLab software (AlFannakh & Ibrahim, 2022).

$$\sigma_{AC} = \sigma_{DC} + A\omega^n \quad (13)$$

where σ_{AC} is AC proton conductivity (S/cm), σ_{DC} is DC proton conductivity (S/cm), A is frequency-dependent constant (S.cm^{n+1}), ω is the angular frequency (rad/s) and n is Power Law exponent ($0 \le n \le 1$).

Degree of Crystallinity

The results of characterization with XRD are in the form of diffractograms that can be used to calculate the degree of crystallinity. Ahmed and Abdullah (2020) mentioned that the calculation of the degree of crystallinity can be done by the deconvolution method using OriginLab software (Ahmed & Abdullah, 2020; Zainuddin et al., 2020). The calculation of the degree of crystallinity uses the following equation:

$$(X_c)\ (\%) = \frac{Ca}{Ca + Aa} \times 100 \quad (14)$$

where X_c is is the degree of crystallinity, A_c is the crystal area, and A_a is the amorphous area.

Mechanical Properties Analysis

The mechanical strength of pure CMCh and ammonium acetate complexed CMCh solid electrolyte membrane was measured using a tensile tester using the ASTM d 882 method. The solid electrolyte membranes were cut into rectangular shapes with a size of 5 cm × 1 cm. Then, the solid electrolyte membrane was tested with a gauge length of 2 cm, a load cell of 10 N, and a test speed of 10 mm/min (Sudiarti et al., 2017; Triandini, 2018).

Crystallinities Analysis

Crystallinity analysis of the solid electrolyte membrane was performed using X-ray diffraction (XRD). The radiation beam was Cu Kα at 2θ with a range of 5 to 80^0 (Ahmed & Abdullah, 2020; Zainuddin et al., 2020).

Thermal Analysis

Thermal stability characterization of solid electrolyte membranes was performed using thermogravimetric analysis (TGA SETARAM Thermal analyzer Labsys Evo S60). The samples were heated from 25 ^{0}C to 600^{0}C at a rate of 10 ^{0}C/min under argon gas flow (Samsudin et al., 2014; Triandini, 2018; H. Yang et al., 2019).

RESULTS AND DISCUSSION

Functional Group Analysis of Chitosan and Carboxymethyl Chitosan

Carboxymethyl chitosan is divided into several types based on its substitution, including O-carboxymethyl chitosan (O-CM-chitosan), N-carboxymethyl chitosan (N-CM-chitosan), N, O-carboxymethyl chitosan (N, O-CM-chitosan), and N,N-carboxymethyl chitosan (N,N-CM-chitosan) (Ellina et al., 2021). To determine the type and validation of the structure, functional group analysis was carried out with FTIR-KBr, which can be seen in **Figure 1.**

The chitosan used as a comparison material is a commercial chitosan. The presence of amine groups in chitosan can be detected from the broadened peak

at 3450 cm^{-1}, which is the stretching vibration of -OH and $-NH_2$ groups with overlapping wavenumbers (Bukzem et al., 2016). Peaks of -CH- stretching and bending vibrations were observed at wave numbers 2920 and 1383 cm^{-1} (Bukzem et al., 2016; Lei et al., 2020). Meanwhile, the wave number 1639 cm^{-1} shows C=O vibrations and 1604 cm^{-1} is a deformed N-H vibration (Lusiana et al., 2014; Müller et al., 2015). However, the presence of N-H vibrations in chitosan has a small intensity, indicating that the amount of amide in chitosan is small.

The peak of C-N and C-H bending vibrations was observed at 1383 cm^{-1} (Morandim-Giannetti et al., 2019; Tzaneva et al., 2017). The ether group (-C-O-C-) vibration connecting the glycosidic ring of chitosan was observed at 1154 cm^{-1} (Pineda et al., 2014; Vaghani et al., 2012). The peak of C- O stretching vibrations originating from within the pyranose ring was observed at 1074 cm^{-1} (Katugampola et al., 2014), while the wave number 556 cm^{-1} showed N-H wagging vibrations (Pineda et al., 2014).

The structure of chitosan and carboxymethyl chitosan differs significantly due to the carboxyl group, resulting in a new peak at 1412 cm^{-1} displaying C-O-H vibrations (Putra et al., 2016; Tzaneva et al., 2017). Two firm peaks at 1600 cm^{-1} and 1412 cm^{-1} indicate carboxymethylation, similar to Palaniselvam et al.'s research (Palaniselvam et al., 2023).

Band broadening was determined using equation 10. The results can be seen in **Figure 2.** The band widening at wavenumber 3435 cm^{-1} initially amounted to 725.253 cm^{-1} in the chitosan sample and widened to 763.646 cm^{-1} in the carboxymethyl chitosan sample. Kurniasih et al. (2012) reported band widening in the -OH and -NH vibrational regions, indicating that carboxymethyl is substituted in both groups (Kurniasih et al., 2012). Band widening was also observed at a wave number of 1600 cm^{-1} initially at 251.564 cm^{-1} in the chitosan sample and widened to 323.888 cm^{-1} in the carboxymethyl chitosan sample with a change in the wavenumber, indicating that carboxymethyl is substituted in the N-H group (Doshi et al., 2017; Lusiana et al., 2014). Based on the results, it can be concluded that the type of carboxymethyl chitosan used in this study is N,O-Carboxymethyl chitosan. The structure can be seen in **Figure 2.**

Functional group analysis on the pure CMCh membrane and AmAc-complexed CMCh membrane was performed using FTIR ATR. Comparison of IR spectra of pure CMCh membrane and CMCh-AmAc membrane (**Figure 3**) revealed the following and summarised in Table 1. No new peaks were formed in the IR spectrum of the AmAc-complexed CMCh membrane, indicating that no new bonds were formed between CMCh and the AmAc salt. However, based on observations, there is a shift in wave numbers towards lower O-H and N-H stretching vibrations from pure CMCh membrane (3369 cm^{-1}) to (3325 cm^{-1}) when AmAc salt is added. The wave number shift also occurs in C=O vibrations from 1583 cm^{-1} in pure CMCh membrane samples to 1579 cm^{-1} when CMCh membranes were added with salt. In C-O-H stretching vibrations, there was also a shift in wavenumber from 1412 cm^{-1} to 1408 cm^{-1}. A wavenumber shift indicates the interaction of complex formation between the host polymer and AmAc salt (Singh et al., 2020).

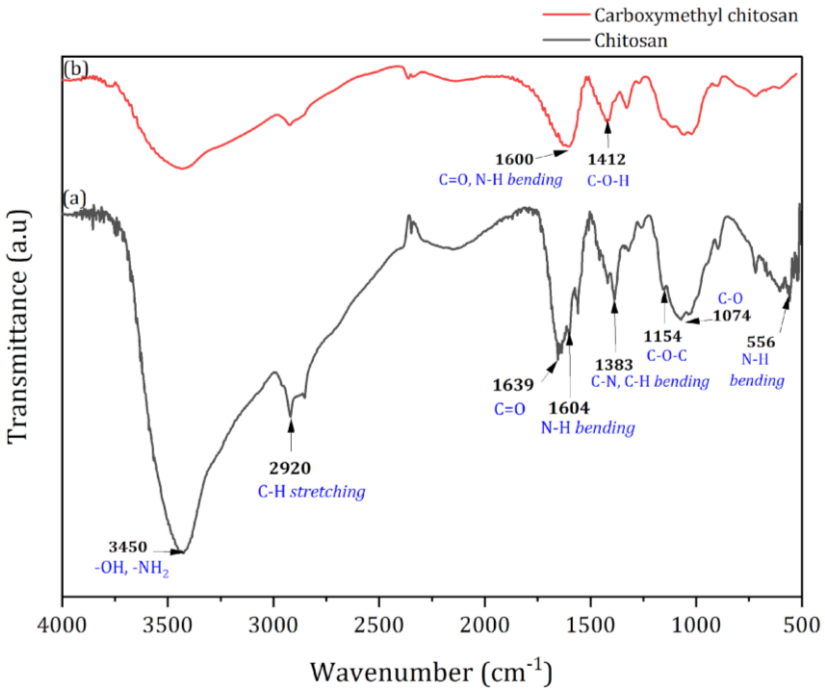

Figure 1. IR spectra of (a) Chitosan and (b) Carboxymethyl Chitosan

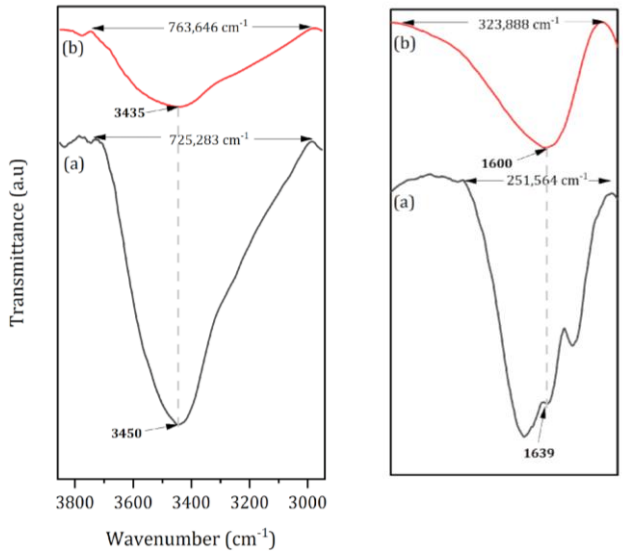

Figure 2. Band Widening in FTIR Analysis of (**a**) Chitosan and (**b**) Carboxymethyl Chitosan

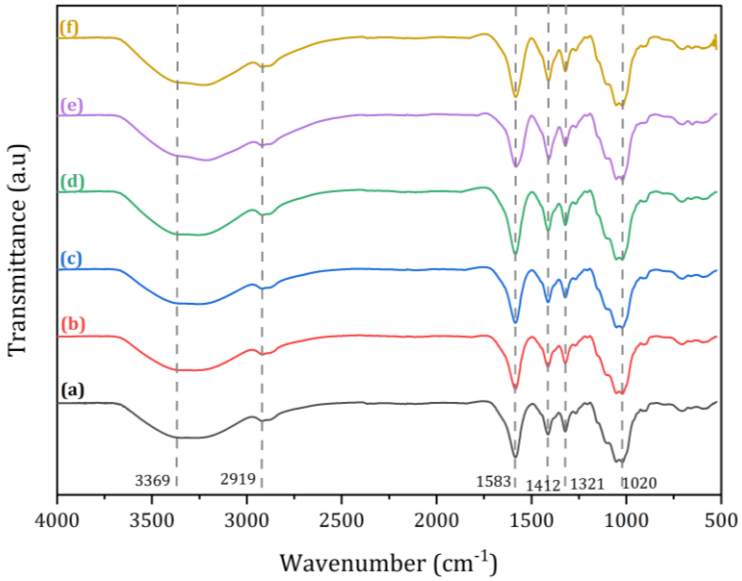

Figure 3. IR Spectra Solid Electrolyte Membranes of (**a**) CMCh, (**b**) CMCh-AmAc (90-10), (**c**) CMCh-AmAc (80-20), (**d**) CMCh-AmAc (70-30), (**e**) CMCh-AmAc (60-40) and (**f**) CMCh-AmAc (50-50)

Table 1. FTIR Analysis of AmAc-Complexed CMCh Solid Electrolyte Membrane

Functional group	Wavenumber (cm^{-1})					
	CMCh	CMCh-AmAc (90-10)	CMCh-AmAc (80-20)	CMCh-AmAc (70-30)	CMCh-AmAc (60-40)	CMCh-AmAc (50-50)
O-H and N-H stretching	3369	3350	3325	3254	3213	3224
C-H ulur	2919	2921	2919	2919	2920	2919
C=O (asam karboksilat)	1583	1583	1583	1583	1579	1581
C-O-H dan N-H bending	1412	1412	1412	1411	1408	1410
C-N stretching	1321	1321	1321	1321	1321	1321
C-O-C (ether)	1020	1020	1020	1020	1019	1019

The C-O-C vibration (1020 cm^{-1}) did not experience a wavenumber shifting. This indicates that the C-O group on the host polymer provides weak Van der Waals interactions with H^+ from the AmAc salt deprotonation process. On the other hand, there is a strong interaction between H^+ from the AmAc salt and the O-H, N-H, and C-O-H functional groups on the CMCh host polymer. These conditions are desirable because these functional groups provide good conducting properties (Rasali et al., 2020; Saadiah et al., 2020).

Complexation formation was also observed in the wavenumber interval of 1500-1700 $cm^{-1,}$ which shows C=O vibrations. In these vibrations, the wavenumber shift did not occur significantly. However, there is a change in intensity **Figure 4**. The change in intensity indicates that there is an interaction between CMCh (oxygen atoms in the carboxyl group) and ammonium ions (free protons) (R et al., 2022; Rasali et al., 2020). Transmittance intensity was calculated with Eq. 11 to determine the effect of salt addition and summarized in **Table 2**; the transmittance intensity changes irregularly. This shows that the transmittance intensity cannot be a reference for the amount of salt in the polymer matrix. This phenomenon is likely due to the membrane's inhomogeneity and thickness, which cannot be controlled in this study. The salt complexation in the electrolyte polymer matrix is also indicated by band broadening; it can be quantified using equation 10. The results of the band widening calculation have been summarized in Table 2, where the widening occurred from 214 to 226 cm^{-1}. According to Gedam & Bhoga (2010), band broadening correlates with adding salt and can form complexes that cause inter-polymer interactions to weaken (Gedam & Bhoga, 2010).

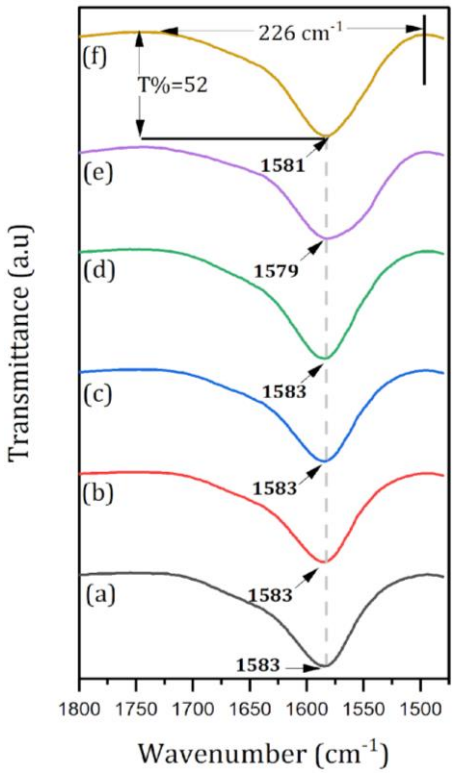

Figure 4. Transmittance Intensity and Band Widening in FTIR Analysis of Solid Electrolyte Membrane

Table 2. Analysis of transmittance intensity and absorption band broadening of AmAc-complexed CMCh solid electrolyte membrane

Sample	T%	1700-1500 cm^{-1} Absorption Band Broadening (cm^{-1})
CMCh	47	209
CMCh-AmAc (90-10)	45	214
CMCh-AmAc (80-20)	46	216
CMCh-AmAc (70-30)	54	221
CMCh-AmAc (60-40)	46	225
CMCh-AmAc (50-50)	52	226

The wavenumber shifting and intensity change can be related to the force constant with Eq. 7-9. The force constant is calculated on the C=O vibration and tabulated in **Table 2**. Based on these data, the CMCh-AmAc (60-40) sample has the smallest force constant value compared to other samples at 100.6 N/cm. As salt is added, the force constant value decreases, indicating that the bond strength decreases. It also shows that the complexation between the polymer and salt increases (Hazaana et al., 2023; Ramalingam et al., 2011).

Molecular Structure Analysis of Carboxymethyl Chitosan

The molecular structure of carboxymethyl chitosan was analyzed using ^{1}H-NMR and ^{13}C-NMR (**Figure 5**). The ^{1}H-NMR spectrum showed a chemical shift at 3.457 ppm, indicating two hydrogens from the carboxymethyl group bound to the nitrogen group (Palaniselvam et al., 2023). Chemical shifts between 3.777 to 3.997 ppm indicate that carboxymethylation occurs in the hydroxyl groups at C-3 and C-6. While carboxymethylation that occurs in the primary amine group shifts at 3.457 ppm (Baari et al., 2021; Kono & Kato, 2021). The signal at 3.77 to 3.997 ppm is a characteristic that indicates that the type of carboxymethyl chitosan substitution is N,O-carboxymethyl chitosan (Jaidee et al., 2012). This ^{1}H-NMR spectrum does not give rise to peaks at 1 to 2 ppm indicating the presence of methyl protons in the acetyl group. This phenomenon indicates that the presence of amide is very little in carboxymethyl chitosan so it does not give rise to chemical shifts in ^{1}H-NMR (Baari et al., 2021).

Figure 5b is the ^{13}C-NMR spectrum of carboxymethyl chitosan. At 72.69 to 76.67 ppm, it shows a methylene carbon group. The O-C-O ring carbon with the numerical C-1 appears at 95.76 to 99.72 ppm. At 71.15 to 71.72 ppm, it shows carbon binding with hydroxyl groups. While carbon binding to the amino group C-N appears in the area of 60.40 to 69.31 ppm (Baari et al., 2021; Sun et al., 2019). Based on the peaks that appear in the ^{13}C-NMR spectrum indicate that the type of carboxymethyl chitosan substitution is N,O-Carboxymethyl chitosan. This became validation data from the initial analysis using FTIR. However, the ^{13}C-NMR spectrum did not show peaks at 170 to 180 ppm, indicating the presence of hydroxyl and amino groups in the carboxymethyl group. This may occur due to the poor solubility factor of N, O-carboxymethyl chitosan with D_2O (Baari et al., 2021).

Table 3. Force Constant of AmAc-Complexed CMCh Solid Electrolyte Membrane

Sample	Functional Group	Vibration Frequency (cm^{-1})	Force Constant (N/cm)
CMCh	C=O	1583	101.1
CMCh-AmAc (90-10)		1583	101.1
CMCh-AmAc (80-20)		1583	101.1
CMCh-AmAc (70-30)		1583	101.1
CMCh-AmAc (60-40)		1579	100.6
CMCh-AmAc (50-50)		1581	100.8

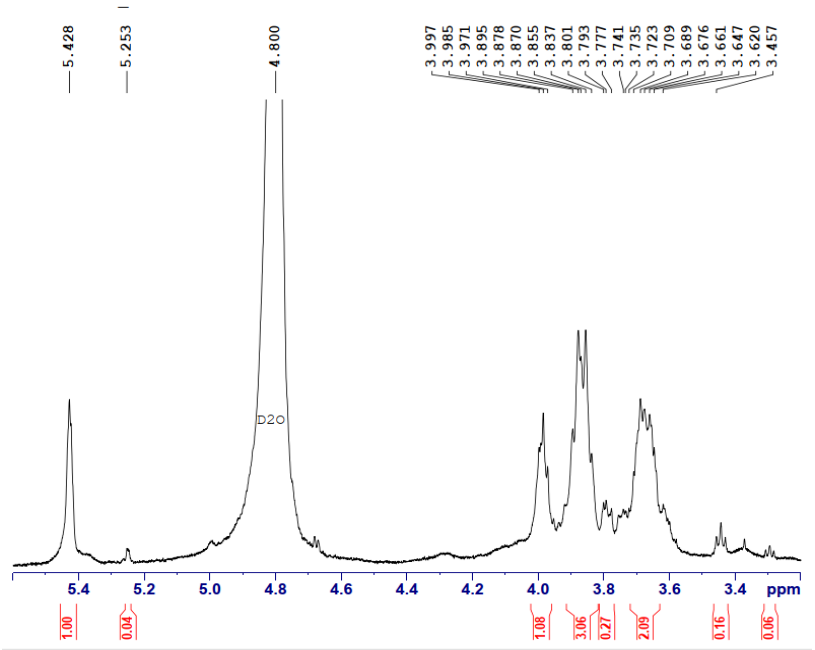

(a)

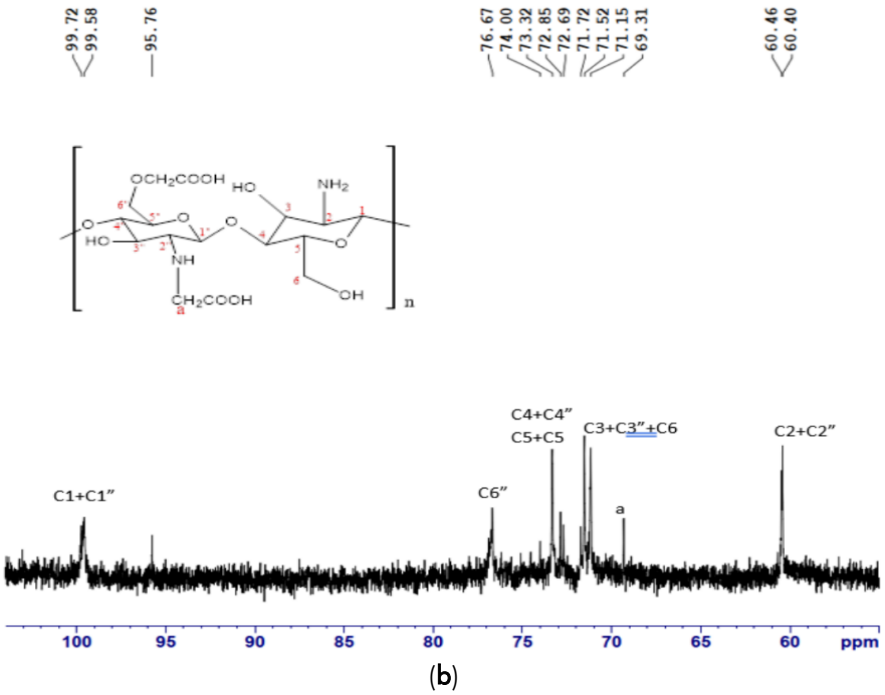

(b)

Figure 5. NMR Spectra Carboxymethyl Chitosan (**a**) ^{1}H-NMR (**b**) ^{13}C-NMR

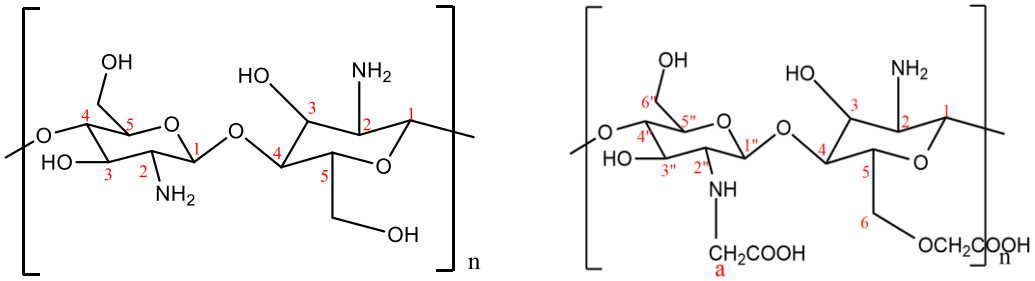

(**a**) (**b**)

Figure 6. Structure (**a**) chitosan dan (**b**) N,O-carboxymethyl chitosan

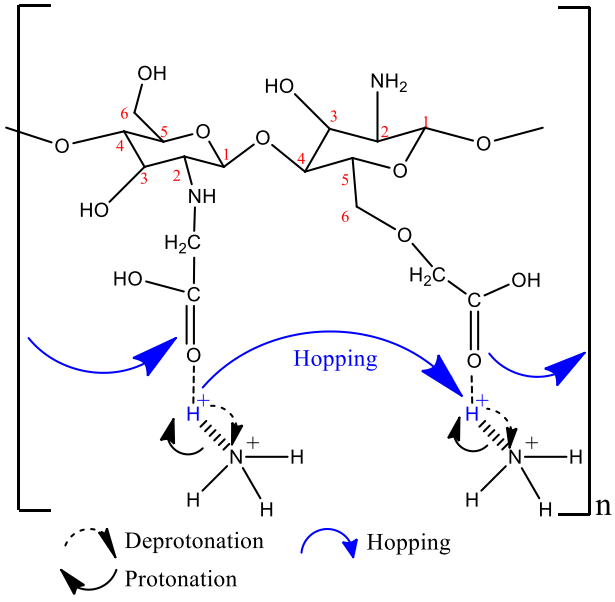

Figure 7. Proposed Mechanism of Proton Hopping on Carboxymethyl Chitosan

Proton transfer in solid electrolyte polymers typically involves proton jumping. Carboxymethyl chitosan, with its polar groups with free electrons, is a transit place for protons before jumping between polar groups. The host polymer's ammonium acetate salt dissociates into ammonium and acetate ions, releasing one hydrogen bond. Protons interact with polar groups on carboxymethyl chitosan, causing movement in the polymer chain. This mechanism is illustrated in **Figure 7**.

Proton Conductivity Analysis

The ion conductivity of the AmAc-complexed CMCh solid electrolyte membrane can be determined by EIS analysis at room temperature. The measurement results with EIS produce a conductance vs frequency graph shown in **Figure 8** and are then processed to obtain DC conductivity using Jonscher's power law equation (Equation 13).

The fitting results (**Table 4**) show that the pure CMCh solid electrolyte membrane has the lowest conductivity value of 1.40×10^{-8} S/cm. However, salt in the CMCh solid electrolyte polymer membrane can increase proton conductivity. The presence of 40% AmAc salt produces the optimum proton conductivity of 7.83×10^{-5} S/cm. Fauzan et al (2020) stated that adding salt to solid electrolyte membranes can increase ion conductivity (Fauzan et al., 2020). This statement aligns with research by Martinez-Cineros et al. (2023). Proton conductivity increases due to amorphous increment as complexation between salt and host polymer consequence. This property facilitates ion mobilization and the movement of polymer chains (Martinez-Cisneros et al., 2023). However, the proton conductivity of the CMCh-AmAc (50-50) variant decreased due to agglomeration, so proton mobility was impaired. Salt concentrations that are too high can also cause ions with polymer chains to have a too tight distance, so ions experience association back into neutral ions (Fauzan et al., 2020).

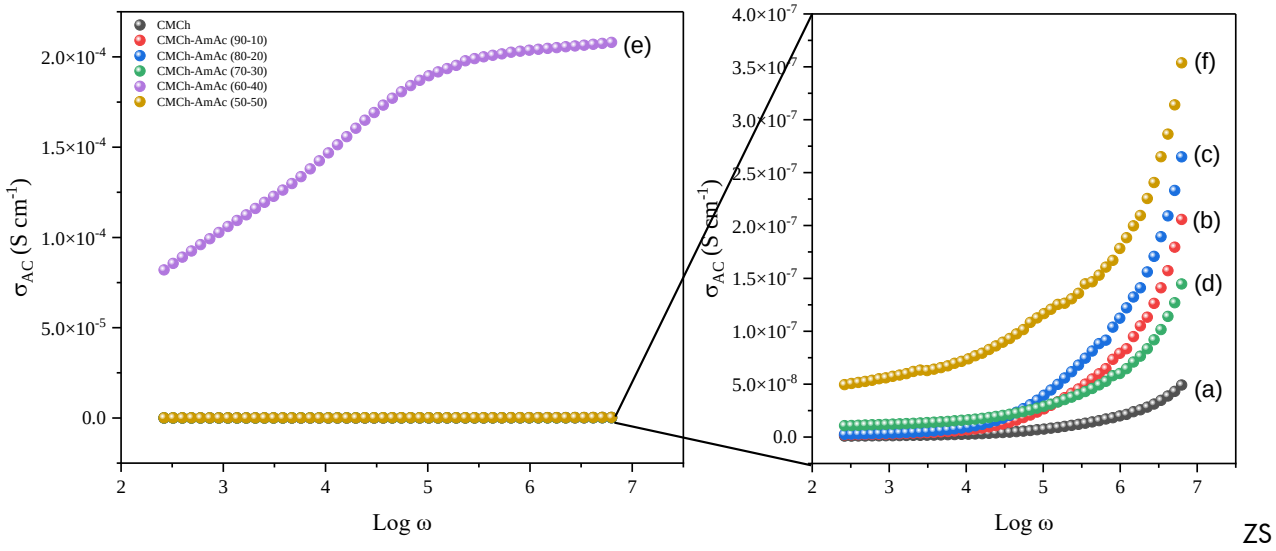

Figure 8. Conductance vs Frequency Curve

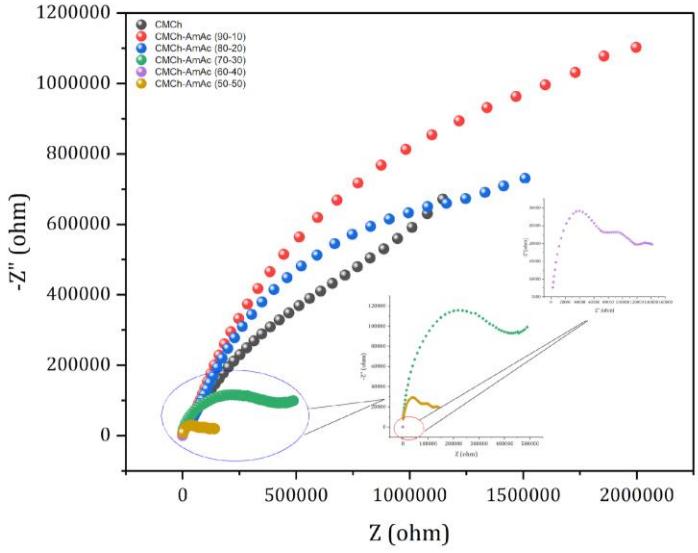

Figure 9. Cole-Cole Curve of CMCh-AmAc Solid Electrolyte Membrane

Table 4. Proton Conductivity of AmAc-Complexed CMCh Solid Electrolyte Membrane

Sample	t (cm)	A (cm^2)	R_{bulk} (ohm)	σ_{DC} (S/cm)	σ_{DC} Proton Bulk (S/cm)
CMCh	0.001	0.785	1.72×10^{3}	1.40×10^{-8}	7.41×10^{-7}
CMCh-AmAc (90-10)	0.004	0.785	2.03×10^{3}	3.34×10^{-8}	2.51×10^{-6}
CMCh-AmAc (80-20)	0.005	0.785	2.63×10^{3}	2.06×10^{-8}	2.42×10^{-6}
CMCh-AmAc (70-30)	0.005	0.785	1.90×10^{3}	4.44×10^{-8}	3.36×10^{-6}
CMCh-AmAc (60-40)	0.006	0.785	5.50×10^{1}	7.83×10^{-5}	1.39×10^{-4}
CMCh-AmAc (50-50)	0.001	0.785	2.42×10^{3}	1.06×10^{-7}	5.26×10^{-7}

Table 5. Free Ions and Contact Ion of AmAc-Complexed CMCh Solid Electrolyte Membrane

Sample	1500-1700 cm^{-1}	
	Free Ions (%)	Contact Ion (%)
CMCh	59.869	40.131
CMCh-AmAc (90-10)	60.080	39.920
CMCh-AmAc (80-20)	60.048	39.952
CMCh-AmAc (70-30)	62.297	37.703
CMCh-AmAc (60-40)	65.195	34.805
CMCh-AmAc (50-50)	63.236	36.764

Measurements with EIS can also produce bulk proton conductivity values using bulk resistance values (Equation 12) obtained from the cole-cole plot shown in **Figure 9**. The highest bulk proton conductivity occurs in the CMCh sample with 40% (w/w) salt addition, which is 1.39×10^{-4} S/cm (summarized in **Table 4**). The phenomenon shows that decreasing bulk resistance causes bulk proton conductivity to increase; this is to the research of Ghani et al (2019). Imperiyka et al. (2013) reported that the decrease in bulk resistance when salt is added is due to the increase of amorphous regions in the solid electrolyte polymer, which facilitates the movement of ions in the polymer faster (Imperiyka et al., 2013).

Percentage of Free Ions and Contact Ions

The dissociation of ammonium acetate salt into cations and anions occurs due to interactions with polar groups on carboxymethyl chitosan. The CMCh sample has smaller free ions due to not adding ammonium acetate salt, while the CMCh-AmAc (60-40) variant has the highest free ion value shown in **Table 5**.

In the CMCh-AmAc (50-50) variant, the free ion is slightly decreased compared to the CMCh-AmAc (60-40) variant. The decrement is occured due to the electrostatic forces so that cations-anions experience association. This phenomenon can be seen from contact ions increment. The ion -pair inhibit the proton to move (Aziz et al., 2020).

Ion Transport Parameters

Table 6 shows that density (η) increases with salt concentration, indicating increased ions in the polymer matrix. The optimum ion mobilization (μ) and diffusion coefficient (D) values are found in solid electrolyte membranes with 40% salt concentration, indicating ion mobility and diffusion coefficient contribute to conductivity. However, an increased acetate salt concentration (50% w/w) increases density, causing high energy required for ion migration due to proton density.

Mechanical Properties Analysis

The study analysis the mechanical properties of solid electrolyte membranes, revealing that salt addition decreases tensile strength and elastic modulus, indicating increased flexibility shown in **Table 7**. The CMCh-AmAc membrane's mechanical properties, influenced by segmental motion, impact conductivity.

Adding 40% (w/w) AmAc salt to electrolyte membranes increases flexibility, segmental motion, and conductivity. However, this also decreases the tensile strength value. Research by Klongkan and Phumcusak (2015) and Wang et al. (2020) shows that salt concentration decreases the tensile strength value (Klongkan & Pumchusak, 2015; Wang et al., 2020). Yulianti et al. (2013) also found that salt reduces the strength of intermolecular forces, affecting the membrane's properties from rigid to flexible. The material's crystallinity also influences these changes (Yulianti et al., 2013). However, when adding 50% AmAc salt, there was an increase in the elastic modulus value (Summarized in **Table 7**). This is due to the re-association to form ammonium acetate salt so that the polymer matrix interaction is strong again.

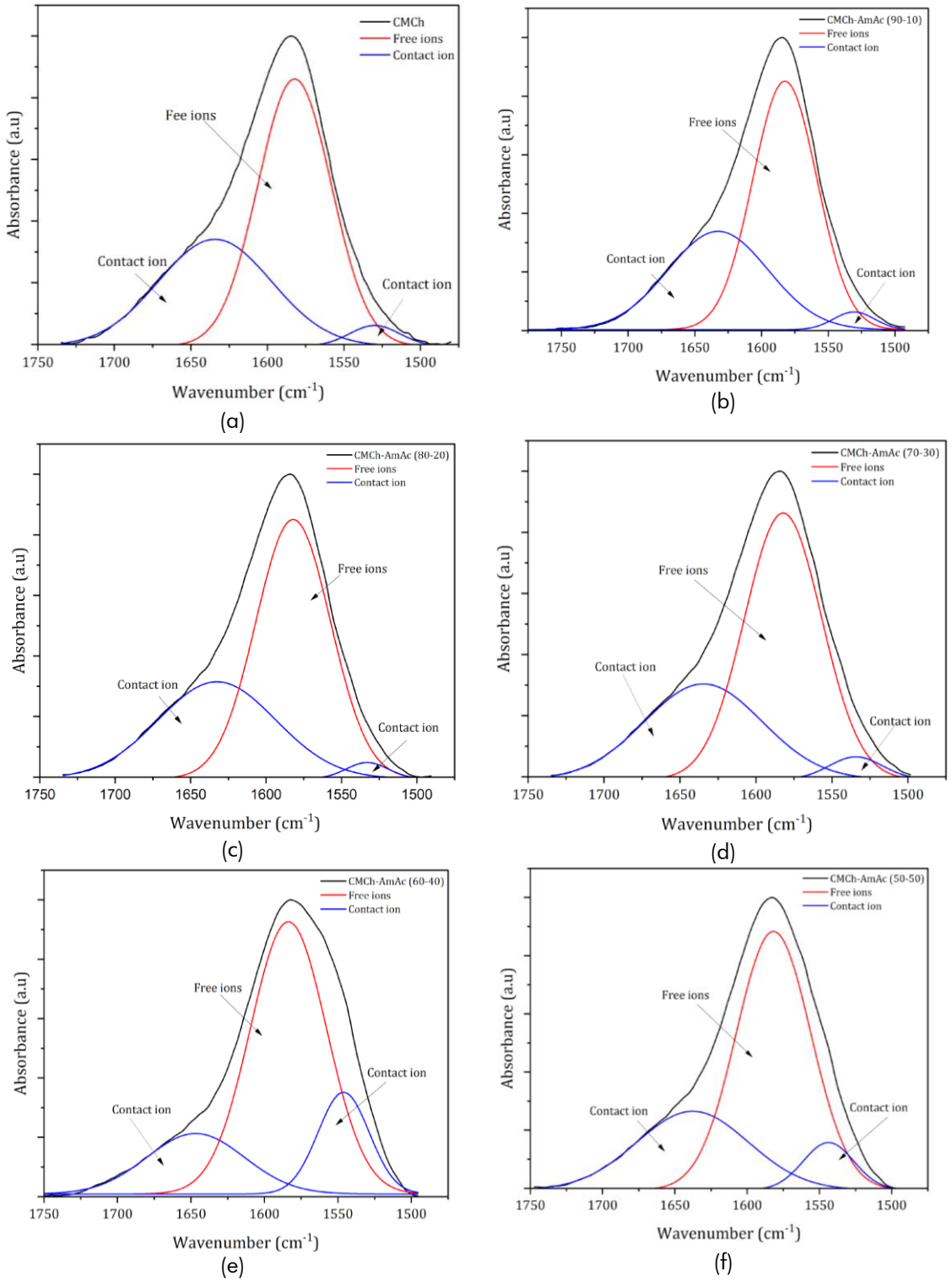

Figure 10. FTIR Deconvolution Curve of Solid Electrolyte Membrane

Table 6. Ion Transport Parameter of AmAc-Complexed CMCh Solid Electrolyte Membrane

Sample	η (cm^{-3})	μ (cm^{-2} $mL^{-1}s^{-1}$)	D (cm^2s^{-1})
CMCh-AmAc (90-10)	1.173×10^{21}	1.337×10^{-8}	3.148×10^{-10}
CMCh-AmAc (80-20)	2.345×10^{21}	6.462×10^{-9}	1.522×10^{-10}
CMCh-AmAc (70-30)	3.649×10^{21}	5.750×10^{-9}	1.354×10^{-10}
CMCh-AmAc (60-40)	5.092×10^{21}	1.707×10^{-7}	4.020×10^{-09}
CMCh-AmAc (50-50)	6.173×10^{21}	5.324×10^{-10}	1.254×10^{-11}

Table 7. Ion transport parameter of AmAc-complexed CMCh solid electrolyte membrane

Sample	Tensile Strength (MPa)	Elongation Break (%)	Elastisitas Modulus (MPa)
CMCh	86.90	7.61	4020
CMCh-AmAc (90-10)	66.65	3.03	3030
CMCh-AmAc (80-20)	64.42	4.04	3860
CMCh-AmAc (70-30)	56.13	7.27	2390
CMCh-AmAc (60-40)	9.06	41.73	50
CMCh-AmAc (50-50)	64.59	6.91	2070

Crystallinity Analysis

X-ray diffraction studies were conducted to investigate the changes in semicrystalline properties of pure CMCh membrane and CMCh-AmAc (60-40) membrane. Sari et al (2016) suggested that the diffraction peak of CMCh is at $2\boldsymbol{\theta}$ = 19° (Sari et al. 2016). Previous research also showed that the CMCh diffraction peaks were at $2\boldsymbol{\theta}$ = 9, 20, 34, 35, and 45°. In this study, the diffraction peak of the CMCh membrane is located at 21.3°, while the diffraction peak of the CMCh-AmAc (60-40) membrane has a peak shift at 18.5°, depicted in **Figure 11**. According to Kumar et al (2017), the shift in the diffractogram peak can occur due to the interaction between the polymer and salt (Kumar et al., 2017). The addition of salt also causes a widening of the diffraction peak and a decrease in intensity, indicating an increase in the amorphous region due to the CMCh host polymer complexing with AmAc.

Adding salt can reduce the degree of crystallinity, which is determined using the deconvolution method and calculated by Equation 14. This is due to structural changes and hydrogen interactions (Wakrim et al., 2023). AmAc salts can form intermolecular coordination in the crystalline area, resulting in more flexible chains. Amorphous areas are preferred in solid electrolyte membrane manufacturing due to their ability to facilitate ion transport and reduce energy barriers for segmental movement (Pandi et al., 2016); (Du et al., 2009; Gedam & Bhoga, 2010; Singh et al., 2020).

Thermal Analysis

The thermal stability of solid electrolyte membranes is crucial for proton battery safety, as it prevents short circuits between the anode and cathode. At 100°C, CMCh and CMCh-AmAC (60-40) membranes evaporated with weight losses of 15.95% and 6.69%, respectively. Adding salt decreases weight degradation due to its hydrophilic properties (Noor et al., 2010). CMCh membranes doped with AmAc salt have lower thermal stability than pure CMCh. The decrease in thermal stability is due to the formation of an amorphous phase between AmAc salt and CMCh polymer cations, which weakens intermolecular interactions (Genier et al., 2019; Jumaah et al., 2015). The DTG curve shows that CMCh membranes show maximum weight loss at 272.29°C (**Table 8**, **Figure 12**), indicating side chain degradation, while CMCh-AmAc (60-40) membranes show structural decomposition. The CMCh membrane has a higher maximum degradation temperature than the CMCh-AmAc (60-40) product, indicating that adding salt can reduce thermal stability.

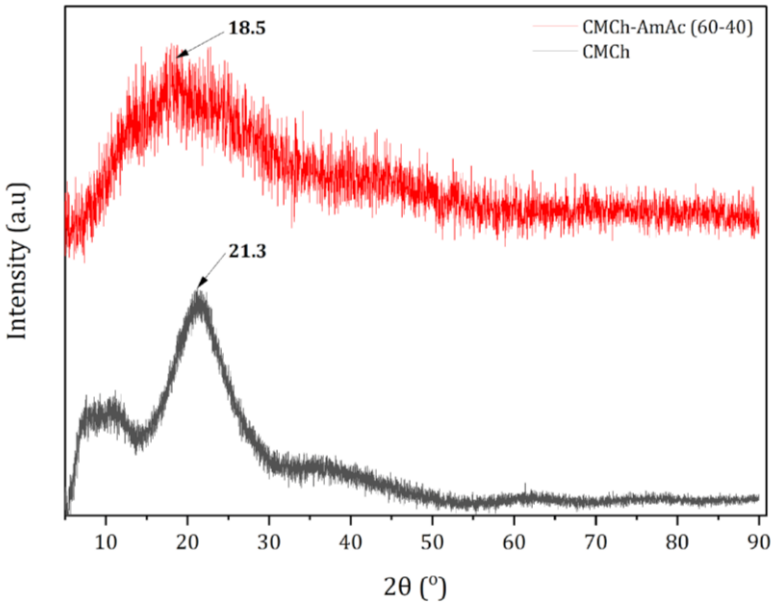

Figure 11. Diffractogram XRD Solid Electrolyte Membrane

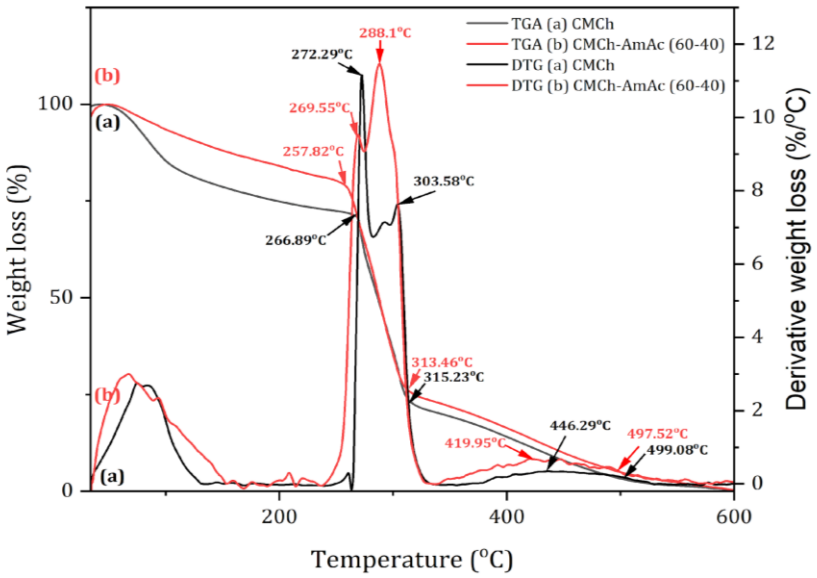

Figure 12. TGA and DTG (**a**) CMCh (**b**) CMCh-AmAc (60-40)

Table 8. Thermal analysis of AmAc-complexed CMCh solid electrolyte membrane

Sample	T_{onset} (°C)	T_{offset} (°C)	$T_{max\ 1}$ (°C)	$T_{max\ 2}$ (°C)
CMCh	266.89	315.23	272.29	303.58
CMCh-AmAc (60-40)	257.82	313.46	269.55	288.1

CONCLUSIONS

The carboxymethyl chitosan-based solid electrolyte membrane complexed with ammonium acetate was successfully prepared using the pour-molding method with variations in the composition of ammonium acetate salts of 0, 10, 20, 30, 40, and 50% (w/w). Based on the research results for all compositions, the solid electrolyte membrane with the best condition is CMCh complexed with AmAc as much as 40% (w/w) and characterized by the highest ionic conductivity value of 1.39×10^{-4} S/cm. However, adding salt decreased the degree of crystallinity, mechanical properties, and thermal stability.

ACKNOWLEDGMENTS

We acknowledge the technicians and analysts from Integrated Chemistry Laboratory, Energy and Materials Engineering Research (Universitas Pertamina), conductivity test technician at BRIN Advanced Materials Research Center, tensile test technician at BRIN Cibinong Biomaterials Research Center, XRD technician at GreenLabs, and TGA technician at BRIN Materials Technology Center.

REFERENCES

Abdalrahman, A. A., Aziz, S. B., & Karim, W. O. (2022). EIS and FTIR approaches to study the ion transport parameters and relaxation dynamics of Na+1 ion in SPE based on MC polymer inserted with sodium salt. *Results in Physics*, *36*. https://doi.org/10.1016/j.rinp.2022.105439

Abdullah, O. Gh., Ahmed, H. T., Tahir, D. A., Jamal, G. M., & Mohamad, A. H. (2021). Influence of PEG plasticizer content on the proton-conducting PEO:MC-NH4I blend polymer electrolytes based films. *Results in Physics*, *23*, 104073. https://doi.org/10.1016/j.rinp.2021.104073

Ahmed, H. T., & Abdullah, O. G. (2020). Structural and ionic conductivity characterization of PEO:MC-NH4I proton-conducting polymer blend electrolytes based films. *Results in Physics*, *16*, 102861. https://doi.org/10.1016/J.RINP.2019.102861

Akhtar, M. N., Khan, A. A., Akhtar, M. N., Ahmad, M., & Khan, M. A. (2019). Structural rietveld refinement, morphological and magnetic features of Cu doped Co–]Ce nanocrystalline ferrites for high frequency applications. *Physica B: Condensed Matter*, *561*, 121–131. https://doi.org/10.1016/j.physb.2019.02.055

AlFannakh, H., & Ibrahim, S. S. (2022). The AC conductivity and dielectric permittivity for PVA-treated MWCNT electrolyte composite. *Journal of Materials Science: Materials in Electronics*, *33*(31), 24137–24150. https://doi.org/10.1007/s10854-022-09092-x

Alias, S. S., Chee, S. M., & Mohamad, A. A. (2017). Chitosan–ammonium acetate–ethylene carbonate membrane for proton batteries. *Arabian Journal of Chemistry*, *10*, S3687–

S3698. https://doi.org/10.1016/j.arabjc.2014.05.001

Aziz, S. B., Asnawi, A. S. F. M., Abdulwahid, R. T., Ghareeb, H. O., Alshehri, S. M., Ahamad, T., Hadi, J. M., & Kadir, M. F. Z. (2021). Design of potassium ion conducting PVA based polymer electrolyte with improved ion transport properties for EDLC device application. *Journal of Materials Research and Technology*, *13*, 933–946. https://doi.org/10.1016/j.jmrt.2021.05.017

Aziz, S. B., Brza, M. A., Saed, S. R., Hamsan, M. H., & Kadir, M. F. Z. (2020). Ion association as a main shortcoming in polymer blend electrolytes based on CS:PS incorporated with various amounts of ammonium tetrafluoroborate. *Journal of Materials Research and Technology*, *9*(3), 5410–5421. https://doi.org/10.1016/j.jmrt.2020.03.067

Baari, M. J., Bundjali, B., & Wahyuningrum, D. (2021). Performance of n,o-carboxymethyl chitosan as corrosion and scale inhibitors in co2 saturated brine solution. *Indonesian Journal of Chemistry*, *21*(4), 954–967. https://doi.org/10.22146/ijc.64255

Babiker, D. M. D., Usha, Z. R., Wan, C., Hassaan, M. M. El., Chen, X., & Li, L. (2023). Recent progress of composite polyethylene separators for lithium/sodium batteries. *Journal of Power Sources*, *564*, 232853. https://doi.org/10.1016/j.jpowsour.2023.232853

Boopathi, G., Pugalendhi, S., Selvasekarapandian, S. ., Premalatha, M., Monisha, S., & Aristatil, G. (2017). Development of proton conducting biopolymer membrane based on agar–agar for fuel cell. *Ionics*, *23*(10), 2781–2790. https://doi.org/10.1007/s11581-016-1876-x

Brza, M. A., Aziz, S. B., Anuar, H., Ali, F., Hamsan, M. H., Kadir, M. F. Z., & Abdulwahid, R. T. (2020). Metal framework as a novel approach for the fabrication of electric double layer capacitor device with high energy density using plasticized Poly(vinyl alcohol): Ammonium thiocyanate based polymer electrolyte. *Arabian Journal of Chemistry*, *13*(10), 7247–7263. https://doi.org/10.1016/j.arabjc.2020.08.006

Bukzem, A. L., Signini, R., dos Santos, D. M., Lião, L. M., & Ascheri, D. P. R. (2016). Optimization of carboxymethyl chitosan synthesis using response surface methodology and desirability function. *International Journal of Biological Macromolecules*, *85*, 615–624. https://doi.org/10.1016/j.ijbiomac.2016.01.017

Cai, T., Yang, Z., Liu, J., Xu, K., Gao, Y., Zhang, F., Yang, X., & Xie, M. (2023). Carboxymethyl chitosan-derived carbon foam with hierarchical pores tuned by potassium tetraborate and potassium carbonate for supercapacitors. *Journal of Energy Storage*, *60*, 106671. https://doi.org/10.1016/j.est.2023.106671

Chandra, A., Chandra, A., & Thakur, K. (2016). Synthesis and ion conduction mechanism on hot-pressed sodium ion conducting nano composite polymer electrolytes. *Arabian Journal of Chemistry*, *9*(3), 400–407. https://doi.org/10.1016/j.arabjc.2013.07.014

Dannoun, E. M. A., Aziz, S. B., Abdulwahid, R. T., Al-Saeedi, S. I., Nofal, M. M., Sadiq, N. M., & Hadi, J. M. (2022). Study of MC:DN-Based Biopolymer Blend Electrolytes with Inserted Zn-Metal Complex for Energy Storage Devices with Improved Electrochemical Performance. *Membranes*, *12*(8), 769. https://doi.org/10.3390/membranes12080769

Doshi, B., Repo, E., Heiskanen, J. P., Sirviö, J. A., & Sillanpää, M. (2017). Effectiveness of N,O-carboxymethyl chitosan on destabilization of Marine Diesel, Diesel and Marine-2T oil for oil spill treatment. *Carbohydrate Polymers*, *167*, 326–336. https://doi.org/10.1016/j.carbpol.2017.03.064

Ellina, N., Salehuddin, A., Rodzali, N. A., Halim, K., Bulat, K., & Mobarak, N. N. (2021). Site-Selective Carboxymethylation of Chitosan Under Heterogeneous Conditions (Penentuan Tapak bagi Proses Pengkarboksimetil pada Kitosan dalam Keadaan Heterogen). *Malaysian Journal of Analytical Sciences*, *25*(3), 376–387.

Fauzan, A. S., Asnawi, M., Hamsan, M. H., & Kadir, M. F. Z. (2020). Electrical and infrared spectroscopic analysis of solid polymer electrolyte based on polyethylene oxide and graphene oxide blend. *Article in Malaysian Journal of Analytical Sciences*, *24*, 682–697. https://www.researchgate.net/publication/344803664

Francis, C. F. J., Kyratzis, I. L., & Best, A. S. (2020). Lithium-Ion Battery Separators for Ionic-Liquid Electrolytes: A Review. In *Advanced Materials* (Vol. 32, Issue 18). Wiley-VCH Verlag. https://doi.org/10.1002/adma.201904205

Gedam, S. K., & Bhoga, S. S. (2010). Preparation and Characterization of Proton Conducting Polymer Electrolyte. *Integrated Ferroelectrics*, *119*(1), 74–81. https://doi.org/10.1080/10584587.2010.490700

Genier, F. S., Burdin, C. V., Biria, S., & Hosein, I. D. (2019). A novel calcium-ion solid polymer electrolyte based on crosslinked poly(ethylene glycol) diacrylate. *Journal of Power Sources*, *414*, 302–307. https://doi.org/10.1016/j.jpowsour.2019.01.017

Ghani, N. A. A., Othaman, R., Ahmad, A., Anuar, F. H., & Hassan, N. H. (2019). Impact of purification on iota carrageenan as solid polymer electrolyte. *Arabian Journal of*

Chemistry, *12*(3), 370–376. https://doi.org/10.1016/j.arabjc.2018.06.008

Guo, L., Ding, Y., Qin, C., Song, W., Sun, S., Fang, K., Li, W., Du, J., & Wang, F. (2018). Anchoring Mn3O4 nanoparticles onto nitrogen-doped porous carbon spheres derived from carboxymethyl chitosan as superior anodes for lithium-ion batteries. *Journal of Alloys and Compounds*, *735*, 209–217. https://doi.org/10.1016/j.jallcom.2017.11.068

Hadi, J. M., Aziz, S. B., Brza, M. A., Kadir, M. F. Z., Abdulwahid, R. T., Ali Al-Asbahi, B., & Ahmed Ali Ahmed, A. (2022). Structural and energy storage behavior of ion conducting biopolymer blend electrolytes based on methylcellulose: Dextran polymers. *Alexandria Engineering Journal*, *61*(12), 9273–9285. https://doi.org/10.1016/j.aej.2022.03.042

Hadi, J. M., Aziz, S. B., Ghafur Rauf, H., Abdulwahid, R. T., Al-Saeedi, S. I., Tahir, D. A., & Kadir, M. F. Z. (2022). Proton conducting polymer blend electrolytes based on MC: FTIR, ion transport and electrochemical studies. *Arabian Journal of Chemistry*, *15*(11), 104172. https://doi.org/10.1016/j.arabjc.2022.104172

Hafiza, M. N., & Isa, M. I. N. (2017). Solid polymer electrolyte production from 2-hydroxyethyl cellulose: Effect of ammonium nitrate composition on its structural properties. *Carbohydrate Polymers*, *165*, 123–131. https://doi.org/10.1016/j.carbpol.2017.02.033

Han, B., Jiang, P., Li, S., & Lu, X. (2021). Functionalized gel polymer electrolyte membrane for high performance Li metal batteries. *Solid State Ionics*, *361*, 115572. https://doi.org/10.1016/j.ssi.2021.115572

Hazaana, S. A., Joseph, A., Selvasekarapandian, S., Naachiyar, R. M., & Vignesh, N. M. (2023). Performance of solid-state Li-ion conducting battery using biopolymer electrolyte based on agar–agar/lithium chloride. *Journal of Solid State Electrochemistry*, *27*(2), 539–557. https://doi.org/10.1007/s10008-022-05348-y

Heidari, S., Seif Mohammadi, S., Oberoi, A. S., & Andrews, J. (2018). Technical feasibility of a proton battery with an activated carbon electrode. *International Journal of Hydrogen Energy*, *43*(12), 6197–6209. https://doi.org/10.1016/j.ijhydene.2018.01.153

Hemalatha, R., Alagar, M., Rameshbabu, P., Azhagu Parvathi, A., & Hepzi Pramila Devamani, R. (2021). Development of medicinal plant (Centella Asiatica – Gotu Kola) based proton conducting polymer electrolytes for electrochemical device applications. *Materials Today: Proceedings*. https://doi.org/10.1016/j.matpr.2021.03.217

Hosseinioun, A., & Paillard, E. (2020). In situ crosslinked PMMA gel electrolyte from a low viscosity precursor solution for cost-effective, long lasting and sustainable lithium-ion batteries. *Journal of Membrane Science*, *594*, 117456. https://doi.org/10.1016/j.memsci.2019.117456

Huy, V. P. H., So, S., & Hur, J. (2021). Inorganic fillers in composite gel polymer electrolytes for high-performance lithium and non-lithium polymer batteries. In *Nanomaterials* (Vol. 11, Issue 3, pp. 1–40). MDPI AG. https://doi.org/10.3390/nano11030614

Imperiyka, M., Ahmad, A., Hanifah, S. A., & Rahman, M. Y. A. (2013). Potential of UV-curable poly(glycidyl methacrylate-co-ethyl methacrylate)-based solid polymer electrolyte for lithium ion battery application. *International Journal of Electrochemical Science*, *8*(9), 10932–10945. https://doi.org/10.1016/s1452-3981(23)13160-9

Jaidee, A., Rachtanapun, P., & Luangkamin, S. (2012). 1H-NMR analysis of degree of substitution in N,O-carboxymethyl chitosans from various chitosan sources and types. *Advanced Materials Research*, *506*, 158–161. https://doi.org/10.4028/www.scientific.net/AMR.506.158

Jian, S., Cao, Y., Feng, W., Yin, G., Zhao, Y., Lai, Y., Zhang, T., Ling, X., Wu, H., Bi, H., & Dong, Y. (2022). Recent progress in solid polymer electrolytes with various dimensional fillers: a review. *Materials Today Sustainability*, *20*, 100224. https://doi.org/10.1016/j.mtsust.2022.100224

Jiang, H., Wu, Y., Ma, J., Liu, Y., Wang, L., Yao, X., & Xiang, H. (2021). Ultrathin polymer-in-ceramic and ceramic-in-polymer bilayer composite solid electrolyte membrane for high-voltage lithium metal batteries. *Journal of Membrane Science*, *640*, 119840. https://doi.org/10.1016/j.memsci.2021.119840

Katugampola, P., Winstead, C., & Adeleke, A. (2014). Thermal stability of carboxymethyl chitosan varying the degree of substitution. *International Journal of Pharmaceutical Science Invention ISSN*, *3*(5), 42–48. www.ijpsi.org

Klongkan, S., & Pumchusak, J. (2015). Effects of Nano Alumina and Plasticizers on Morphology, Ionic Conductivity, Thermal and Mechanical Properties of PEO-LiCF3SO3 Solid Polymer Electrolyte. *Electrochimica Acta*, *161*, 171–176. https://doi.org/10.1016/j.electacta.2015.02.074

Kono, H., & Kato, T. (2021). Elucidation of substituent distribution states for carboxymethyl chitosan by detailed NMR analysis. *Carbohydrate Polymer Technologies and Applications*, *2*. https://doi.org/10.1016/j.carpta.2021.100175

Kurniasih, M., Kartika, D., & Riyanti. (2012). Sintesis dan Karakterisasi Karboksimetil Kitosan. *Prosiding Seminar Nasional LPPM Unsoed*, 125–132.

Lakshmi, K. C. S., Ji, X., Chen, T.-Y., Vedhanarayanan, B., & Lin, T.-W. (2021). Pseudocapacitive and battery-type organic polymer electrodes for a 1.9 V hybrid supercapacitor with a record concentration of ammonium acetate. *Journal of Power Sources*, *511*, 230434. https://doi.org/10.1016/j.jpowsour.2021.230434

Lei, M., Huang, W., Sun, J., Shao, Z., Duan, W., Wu, T., & Wang, Y. (2020). Synthesis, characterization, and performance of carboxymethyl chitosan with different molecular weight as additive in water-based drilling fluid. *Journal of Molecular Liquids*, *310*. https://doi.org/10.1016/j.molliq.2020.113135

Li, Y., Yang, Y., Liu, X., Yang, Y., Wu, Y., Han, L., & Han, Q. (2022). Flexible self-powered integrated sensing system based on a rechargeable zinc-ion battery by using a multifunctional polyacrylamide/carboxymethyl chitosan/LiCl ionic hydrogel. *Colloids and Surfaces A: Physicochemical and Engineering Aspects*, *648*, 129254. https://doi.org/10.1016/j.colsurfa.2022.129254

Lizundia, E., & Kundu, D. (2021). Advances in Natural Biopolymer-Based Electrolytes and Separators for Battery Applications. In *Advanced Functional Materials* (Vol. 31, Issue 3). Wiley-VCH Verlag. https://doi.org/10.1002/adfm.202005646

Lusiana, R. A., Siswanta, D., & Mudasir. (2014). Modifying Surface Charge of Chitosan Membrane by N,O-Carboxymethyl chitosan Blended with Poly(vinylalcohol). *International Journal of Advances in Chemical Engineering and Biological Sciences*, *1*(1). https://doi.org/10.15242/ijacebs.c1113034

Mahalakshmi, M., Selvanayagam, S., Selvasekarapandian, S., Moniha, V., Manjuladevi, R., & Sangeetha, P. (2019). Characterization of biopolymer electrolytes based on cellulose acetate with magnesium perchlorate (Mg(ClO4)2) for energy storage devices. *Journal of Science: Advanced Materials and Devices*, *4*(2), 276–284. https://doi.org/10.1016/j.jsamd.2019.04.006

Manoharan, S., Pazhamalai, P., Mariappan, V. K., Murugesan, K., Subramanian, S., Krishnamoorthy, K., & Kim, S.-J. (2021). Proton conducting solid electrolyte-piezoelectric PVDF hybrids: Novel bifunctional separator for self-charging supercapacitor power cell. *Nano Energy*, *83*, 105753. https://doi.org/10.1016/j.nanoen.2021.105753

Martinez-Cisneros, C. S., Pandit, B., Levenfeld, B., Varez, A., & Sanchez, J.-Y. (2023). Flexible solvent-free polymer electrolytes for solid-state Na batteries. *Journal of Power Sources*, *559*, 232644. https://doi.org/10.1016/j.jpowsour.2023.232644

Mejenom, A. A., Hafiza, M. N., & Isa, M. I. N. (2018). X-Ray Diffraction and Infrared Spectroscopic Analysis of Solid Biopolymer Electrolytes Based on Dual Blend Carboxymethyl Cellulose-Chitosan Doped with Ammonium Bromide. In *ASM Sci. J.Special Issue* (Vol. 2018, Issue 1).

Miao, J., Li, L., Guohua, C., Congjie, G., & Shengxiong, D. (2008). Preparation of N, O-carboxymethyl Chitosan Composite Nanofiltration Membrane and Its Rejection Performance for the Fermentation Effluent from a Wine Factory *. In *Chinese Journal of Chemical Engineering* (Vol. 16, Issue 2).

Morandim-Giannetti, A. de A., Wecchi, P. de O., Silvério, P. de A., Carlstron, R., & Bersanetti, P. A. (2019). Attainment and characterization of carboxymethyl chitosan hydrogels by enzymatic cross-linking. *Journal of Thermal Analysis and Calorimetry*, *138*(5), 3635–3643. https://doi.org/10.1007/s10973-019-08571-4

Müller, W. E. G., Neufurth, M., Tolba, E., Schröder, H. C., Wang, S., Link, T., Al-Nawas, B., & Wang, X. (2015). A new printable and durable N,O-carboxymethyl chitosan-Ca 2+-polyphosphate complex with morphogenetic activity. *Journal of Material Chemistry B*, *3*, 1722–1730. https://doi.org/https://doi.org/10.1039/C4TB01586J

Nayla, M., & Radiman, C. L. (2023). Pengaruh Konsentrasi Agen Pensulfonasi Terhadap Karakteristik Membran Selulosa Bakterial Tersulfonasi Pada Aplikasi DMFC. *ALCHEMY:Journal of Chemistry*, *10*(2), 60–70. https://doi.org/10.18860/al.v10i2.13519

Noor, S. A. M., Ahmad, A., Talib, I. A., & Rahman, M. Y. A. (2010). Morphology, chemical interaction, and conductivity of a PEO-ENR50 based on solid polymer electrolyte. *Ionics*, *16*(2), 161–170. https://doi.org/10.1007/s11581-009-0385-6

Nuryanto, R., Suyati, L., Harjono, C., & Anggrayni, R. (2013). Pengaruh Konsentrasi Kalium Asetat dan Natrium Asetat terhadap Konduktivitas Elektrolit Padat KMn(2-x)MgxO2 dan NaMn(2-x)MgxO2. *Jurnal Sains Dan Matematika*, *21*(2), 35–38.

Pahune, B. S. (2011). Synthesis and Characterization of Proton Exchange Membrane for Fuel Cell Technology. *Archives of Applied Science Research*, *3*(4), 78–82. www.scholarsresearchlibrary.com

Palaniselvam, S., Vijayanand, R., Selvachandhran, V., Manase, S., Rajagopal, S. K., & Ramachandran, S. (2023). Structural characterization and toxicity effect of nano-carboxymethyl chitosan from Uroteuthis

(Photololigo) sibogae (Adam, 1954) in the zebrafish model. *Biomass Conversion and Biorefinery*. https://doi.org/10.1007/s13399-023-04480-7

Pandi, D. V., Selvasekarapandian, S., Bhuvaneswari, R., Premalatha, M., Monisha, S., Arunkumar, D., & Junichi, K. (2016). Development and characterization of proton conducting polymer electrolyte based on PVA, amino acid glycine and NH4SCN. *Solid State Ionics*, *298*, 15–22. https://doi.org/10.1016/j.ssi.2016.10.016

Pineda, M. G., Torres, S., López, L. V., Enríquez-Medrano, F. J., De León, R. D., Fernández, S., Saade, H., & López, R. G. (2014). Chitosan-coated magnetic nanoparticles prepared in one-step by precipitation in a high- Aqueous phase content reverse microemulsion. *Molecules*, *19*(7), 9273–9287. https://doi.org/10.3390/molecules19079273

Pratiwi, D. E. (2018). *Sintesis Membran Elektrolit Padat Berbahan Dasar Kitosan: Vol. VII* (Issue 2). Cetak. http://ojs.unm.ac.id/index.php/sainsmat86

Putra, P., Husni, A., & Dewi Puspita, I. (2016). Characterization and Application of N,O-Carboxy Methyl Chitosan Produced at Different Tempererature of Etherification. *International Journal of Pharmaceutical and Clinical Research*, *8*(11), 1493–1498. www.ijpcr.com

Putri, R. M., Floweri, O., Mayangsari, T. R., Aimon, A. H., & Iskandar, F. (2021). Preliminary study of electrochemical properties of polyethylene oxide (PEO) and polyvinyl alcohol (PVA) composites as material for solid polymer electrolyte. *Materials Today: Proceedings*, *44*, 3375–3377. https://doi.org/10.1016/j.matpr.2020.11.663

Qiu, Z., Shi, L., Wang, Z., Mindemark, J., Zhu, J., Edström, K., Zhao, Y., & Yuan, S. (2019). Surface activated polyethylene separator promoting Li+ ion transport in gel polymer electrolytes and cycling stability of Li-metal anode. *Chemical Engineering Journal*, *368*, 321–330. https://doi.org/10.1016/j.cej.2019.02.107

R, M. N., M, R., S, S., G, A., S, A. H., N, M. V., & M, V. K. (2022). Fabrication of rechargeable proton battery and PEM fuel cell using biopolymer Gellan gum incorporated with NH4HCO2 solid electrolyte. *Journal of Polymer Research*, *29*(8), 337. https://doi.org/10.1007/s10965-022-03190-4

Rahamathullah, R., Khairul, W. M., & Isa, M. I. N. (2020). Contribution of stilbene-imine additives on the structural, ionic conductivity performance and theoretical evaluation on CMC-based biopolymer electrolytes. *Carbohydrate Polymers*, *250*, 116935. https://doi.org/10.1016/j.carbpol.2020.116935

Ramalingam, P., Priyadharsini, P., Chandrasekaran, G., Parameshwari, R., & Priyadarshini, P. (2011). Optimization, structural, spectroscopic and magnetic studies on stable akaganeite nanoparticles via co-precipitation method. *American Journal of Materials Science*, *1*(1), 18–25. http://journal.sapub.org/materials

Rasali, N. M. J., Saadiah, M. A., Zainuddin, N. K., Nagao, Y., & Samsudin, A. S. (2020). Ionic transport studies of solid bio-polymer electrolytes based on carboxymethyl cellulose doped with ammonium acetate and its potential application as an electrical double layer capacitor. *Express Polymer Letters*, *14*(7), 619–637. https://doi.org/10.3144/expresspolymlett.2020.51

Saadiah, M. A., Nagao, Y., & Samsudin, A. S. (2020). Proton (H+) transport properties of CMC–PVA blended polymer solid electrolyte doped with NH4NO3. *International Journal of Hydrogen Energy*, *45*(29), 14880–14896. https://doi.org/10.1016/j.ijhydene.2020.03.213

Samsudin, A. S., Lai, H. M., & Isa, M. I. N. (2014). Biopolymer Materials Based Carboxymethyl Cellulose as a Proton Conducting Biopolymer Electrolyte for Application in Rechargeable Proton Battery. *Electrochimica Acta*, *129*, 1–13. https://doi.org/10.1016/j.electacta.2014.02.074

Schlemmer, W., Selinger, J., Hobisch, M. A., & Spirk, S. (2021). Polysaccharides for sustainable energy storage – A review. *Carbohydrate Polymers*, *265*. https://doi.org/10.1016/j.carbpol.2021.118063

Shamsudin, I. J., Shrgawi, N., Hanibah, H., Hassan, N. H., & Ahmad, A. (2020). Carboxymethyl Chitosan-based Biopolymer Electrolyte with Imidazolium Ionic Liquid. *Malaysian Journal of Analytical Sciences*, *24*(5), 744–756.

Sihombing, Y. A., Susilawati, Rahayu, S. U., & Situmeang, M. D. (2023). Effect of reduced graphene oxide (rGO) in chitosan/Pahae natural zeolite-based polymer electrolyte membranes for direct methanol fuel cell (DMFC) applications. *Materials Science for Energy Technologies*, *6*, 252–259. https://doi.org/10.1016/j.mset.2023.01.002

Singh, C., Shukla, P., & Agrawal, S. (2020). Ion transport studies in PVA:NH4CH3COO gel polymer electrolytes. *High Performance Polymers*, *32*(2), 208–219. https://doi.org/10.1177/0954008319898242

Singh Syali, M., Mishra, K., Kanchan, D. K., & Kumar, D. (2021). Studies on a novel Na+ superionic conducting polymer gel cocktail electrolyte membrane immobilizing molecular liquid mixture of carbonates, tetraglyme and ionic liquid. *Journal of Molecular Liquids*, *341*,

116922. https://doi.org/10.1016/j.molliq.2021.116922

Sudiarti, T., Wahyuningrum, D., Bundjali, B., & Made Arcana, I. (2017). Mechanical strength and ionic conductivity of polymer electrolyte membranes prepared from cellulose acetate-lithium perchlorate. *IOP Conference Series: Materials Science and Engineering*, *223*, 012052. https://doi.org/10.1088/1757-899X/223/1/012052

Sun, X., Zhang, J., Chen, Y., Mi, Y., Tan, W., Li, Q., Dong, F., & Guo, Z. (2019). SYnthesis, characterization, and the antioxidant activity of carboxymethyl chitosan derivatives containing thiourea salts. *Polymers*, *11*(11). https://doi.org/10.3390/polym11111810

Suseno, N., SPadmawijaya, K., Welly Wirana, J., & Julio, M. (2017). *Pengaruh Berat Molekul Kitosan terhadap Kelarutan Karboksimetil Kitosan*.

Tahir, H. B., Abdullah, R. M., & Aziz, S. B. (2022). The H+ ion transport study in polymer blends incorporated with ammonium nitrate: XRD, FTIR, and electrical characteristics. *Results in Physics*, *42*, 105960. https://doi.org/10.1016/j.rinp.2022.105960

Triandini, N. W. P. (2018). *Sintesis dan Modifikasi Kitosan dari Limbah Cangkang Udang untuk Eletrolit Padat Baterai Litium*. Institut Teknologi Bandung.

Tzaneva, D., Simitchiev, A., Petkova, N., Nenov, V., Stoyanova, A., & Denev, P. (2017). Synthesis of carboxymethyl chitosan and its rheological behaviour in pharmaceutical and cosmetic emulsions. *Journal of Applied Pharmaceutical Science*, *7*(10), 70–78. https://doi.org/10.7324/JAPS.2017.71010

Vaghani, S. S., Patel, M. M., Satish, C. S., Patel, K. M., & Jivani, N. P. (2012). Synthesis and characterization of carboxymethyl chitosan hydrogel: Application as site specific delivery for lercanidipine hydrochloride. *Bull. Mater. Sci*, *35*(7), 1133–1142.

Varzi, A., Raccichini, R., Passerini, S., & Scrosati, B. (2016). Challenges and prospects of the role of solid electrolytes in the revitalization of lithium metal batteries. *Journal of Materials Chemistry A*, *4*(44), 17251–17259. https://doi.org/10.1039/c6ta07384k

Wakrim, H., Bouftou, A., Aghmih, K., Boukhriss, A., Bouchti, M. El, Saoiabi, S., Gmouh, S., & Majid, S. (2023). Performance evaluation of polymer electrolyte membranes based on hydrogen sulfite ionic liquid for application in direct methanol fuel cell (DMFC). *Journal of Ionic Liquids*, *3*(2), 100063. https://doi.org/10.1016/j.jil.2023.100063

Xie, W., Wu, L., Liu, W., Dang, Y., Tang, A., & Luo, Y. (2021). Modelling electrolyte-immersed tensile property of polypropylene separator for lithium-ion battery. *Mechanics of Materials*, *152*, 103667. https://doi.org/10.1016/j.mechmat.2020.103667

Xu, T., Wang, D., Li, Z., Chen, Z., Zhang, J., Hu, T., Zhang, X., & Shen, L. (2022). Electrochemical Proton Storage: From Fundamental Understanding to Materials to Devices. *Nano-Micro Letters*, *14*(1), 126. https://doi.org/10.1007/s40820-022-00864-y

Yang, H., Liu, Y., Kong, L., Kang, L., & Ran, F. (2019). Biopolymer-based carboxylated chitosan hydrogel film crosslinked by HCl as gel polymer electrolyte for all-solid-sate supercapacitors. *Journal of Power Sources*, *426*, 47–54. https://doi.org/10.1016/j.jpowsour.2019.04.023

Yang, J.-L., Cao, J.-M., Zhao, X.-X., Zhang, K.-Y., Zheng, S.-H., Gu, Z.-Y., & Wu, X.-L. (2022). Advanced aqueous proton batteries: working mechanism, key materials, challenges and prospects. *EnergyChem*, *4*(6), 100092. https://doi.org/10.1016/j.enchem.2022.100092

Yao, P., Yu, H., Ding, Z., Liu, Y., Lu, J., Lavorgna, M., Wu, J., & Liu, X. (2019). Review on Polymer-Based Composite Electrolytes for Lithium Batteries. In *Frontiers in Chemistry* (Vol. 7). Frontiers Media S.A. https://doi.org/10.3389/fchem.2019.00522

Yuan, C., Hahn, Y., Lu, W., Oancea, V., & Xu, J. (2022). Quantification of electrochemical-mechanical coupling in lithium-ion batteries. *Cell Reports Physical Science*, *3*(101158). https://doi.org/10.1016/j.xcrp.2022.101158

Yusof, Y. M., Shukur, M. F., Illias, H. A., & Kadir, M. F. Z. (2014). Conductivity and electrical properties of corn starch-chitosan blend biopolymer electrolyte incorporated with ammonium iodide. *Physica Scripta*, *89*(3). https://doi.org/10.1088/0031-8949/89/ 03/035701

Zainuddin, N. K., Rasali, N. M. J., Mazuki, N. F., Saadiah, M. A., & Samsudin, A. S. (2020). Investigation on favourable ionic conduction based on CMC-K carrageenan proton conducting hybrid solid bio-polymer electrolytes for applications in EDLC. *International Journal of Hydrogen Energy*, *45*(15), 8727–8741. https://doi.org/10.1016/j.ijhydene.2020.01.038

Zhu, F., Ho-Sum Cheng, S., Xu, Y., Liao, W., He, K., Chen, D., Liao, C., Cheng, X., Tang, J., Li, R. K. Y., & Liu, C. (2021). Dual-salt effect on polyethylene oxide/Li6.4La3Zr1.4Ta0.6O12 composite electrolyte for solid-state lithium metal batteries with superior electrochemical performance. *Composites Science and Technology*, *210*, 108837. https://doi.org/10.1016/j.compscitech.2021.108837